inorganics

MDPI

Article

Lewis Base Complexes of Magnesium Borohydride: Enhanced Kinetics and Product Selectivity upon Hydrogen Release

Marina Chong [1], Tom Autrey [1,2,*] and Craig M. Jensen [2,*]

1 Pacific Northwest National Laboratory, 902 Battelle Blvd, Richland, WA 99352, USA; marinac628@gmail.com
2 Department of Chemistry, University of Hawaii at Manoa, 2545 McCarthy Mall, Honolulu, HI 96822, USA
* Correspondence: tom.autrey@pnnl.gov (T.A.); Jensen@hawaii.edu (C.M.J.);
Tel.: +1-509-375-3792 (T.A.); +1-808-956-2769 (C.M.J.)

Received: 3 November 2017; Accepted: 28 November 2017; Published: 6 December 2017

Abstract: Tetrahydofuran (THF) complexed to magnesium borohydride has been found to have a positive effect on both the reactivity and selectivity, enabling release of H_2 at <200 °C and forms $Mg(B_{10}H_{10})$ with high selectivity.

Keywords: hydrogen storage; Lewis base adducts; borohydride

1. Introduction

Over the past decade, there has been a significant international effort involving chemists, materials scientists and physicists to discover and demonstrate a solid-state hydrogen storage material that would enable a fuel cell electric vehicle 5 min refueling time and a 500 km driving range. Only a few of the thousands of materials investigated have garnered as much interest as $Mg(BH_4)_2$ [1–12]. The high gravimetric density of H_2, ca. 14.7 wt % H_2 and thermodynamics for H_2 release lie in the narrow window required for reversibility under moderate pressure and temperature. The dehydrogenation of the borohydride to MgB_2 has a calculated ΔH_0 of 38.6 kJ/(mol H_2) and ΔS of 111.5 J/(K·mol H_2), predicting a plateau pressure of 1 bar H_2 of 73 °C [13]. These thermodynamic properties together with the borohydride's high gravimetric hydrogen density, and demonstrated hydrogen cycling compatibility [1,9] suggest its application as a reversible hydrogen carrier for PEM fuel cell applications. Two critical challenges remaining are (i) the slow rates of hydrogen release and (ii) the thermodynamic stability of the major dehydrogenation product, magnesium dodecaborane, $Mg(B_{12}H_{12})$, occasionally referred to as the dead-end for reversibility.

At temperatures greater than 460 °C the borohydride releases ~14 wt % hydrogen, giving mixture of products, i.e., MgB_2, MgH_2, Mg and amorphous boron, depending on reaction conditions [6,10,11,14,15]. Hydrogenation of this product mixture at 400 bar H_2 and 270 °C results in the uptake of 6.1 wt % hydrogen [5]. NMR studies concluded that $MgB_{12}H_{12}$, forming at temperatures greater than 250 °C, is a thermodynamic endpoint, preventing re-hydrogenation to $Mg(BH_4)_2$ [4]. On the other hand, the reversal of MgB_2 to $Mg(BH_4)_2$ occurs, albeit, under extreme conditions of 950 bar H_2 and 400 °C [9]. This demonstrated that reversibility can be achieved, however, under conditions that are impractical for commercial hydrogen storage applications. Similarly, the lithium, sodium, and potassium salts of $B_{12}H_{12}^{2-}$ have been hydrogenated, in the presence of metal hydrides, to the corresponding borohydride under 1000 bar of H_2 at 500 °C [16]. Whether the pathway for the hydrogenation of MgB_2 to $Mg(BH_4)_2$ involves $MgB_{12}H_{12}$ remains an open question.

The use of additives to enhance kinetics of hydrogen release from $Mg(BH_4)_2$ has been the subject of several investigations [17–20]. An early study found that $TiCl_3$ lowered the onset temperature of hydrogen release from 262 to 88 °C [17]. More recently, significant reductions in the onset temperature

of hydrogen release have been observed upon the addition of $NbCl_5$ and a Ti–Nb nanocomposite [18]; metal fluorides such as CaF_2, ZnF_2, TiF_3, and NbF_5 [18–20] and $ScCl_3$ [19]. Hydrogen release is also induced by mechanically milling $Mg(BH_4)_2$ with TiO_2 resulting in release of 2.4 wt % H_2 at 271 °C while undergoing reversible dehydrogenation to $Mg(B_3H_8)_2$ [20]. Alternatively, the thermal dehydrogenation of $Mg(BH_4)_2$ has been shown to be accelerated in eutectic mixtures with $LiBH_4$ [21–23]. Another study claimed that the addition of LiH to $Mg(BH_4)_2$ induced hydrogen evolution at temperatures as low as 150 °C and enabled the cycling of 3.6 wt % H_2 through 20 cycles at 180 °C [24].

2. Results

The high temperature and pressure required for reversibility led us to explore the decomposition pathways at lower temperatures. The decomposition of $Mg(BH_4)_2$ over a prolonged period (5 weeks) under 1 bar nitrogen at 200 °C yields $Mg(B_3H_8)_2$ as the major product [1]. While formation of the $B_3H_8^-$ anion has been recognized from thermal condensation studies of BH_4^- in solution [25], this finding provided evidence that an analogous process may take place during solid state decomposition contrary to theoretical predictions. Furthermore, under 120 bar hydrogen pressure and 250 °C, the $Mg(B_3H_8)_2$ intermediate was completely converts back to $Mg(BH_4)_2$ after 48 h. The subsequent hydrogenation of independently synthesized $Mg(B_3H_8)_2$·THF (THF = tetrahydofuran), where attempts to remove the solvent were unsuccessful, then demonstrated that quantitative re-hydrogenation to $Mg(BH_4)_2$ could be achieved under 50 bar H_2 and 5 h at 200 °C [26]. We concluded that the faster rate exhibited by the solvated sample resulted from a phase change induced by the coordination of the THF. Studies of borohydrides and boranes in the context of hydrogen storage, have typically focused on complete solvent removal. The presence of residual solvent is generally considered problematic and the various synthetic routes to $Mg(BH_4)_2$ often call for rigorous efforts to obtain a pure, solvent-free product. However, our findings suggested that the solvent coordination might have the beneficial effect of enhancing dehydrogenation kinetics. Only a handful of studies have explored the dehydrogenation of $Mg(BH_4)_2$ coordinated to a solvent, the majority of which have highlighted nitrogen donors [27–30].

Our observation of the kinetic enhancement of the hydrogenation of $Mg(B_3H_8)_2$ to $Mg(BH_4)_2$ prompted us to further explore how solvent coordination affects hydrogen release temperatures. We have examined the effect of dimethyl sulfide (DMS), diethyl ether (Et_2O), triethylamine (TEA), diglyme (Digly), dimethoxy ethane (DME) and THF, encompassing a range of Lewis basicity, on the decomposition of $Mg(BH_4)_2$. Alternative syntheses, complex polymorphism, predicted thermodynamic properties, and attempts to improve the hydrogen cycling capacity of $Mg(BH_4)_2$ have been widely explored and reviews of these activities were recently published [20,31]. However, the solid-state chemistry of the interconversion of the borane intermediates involved in these systems remains largely unexplored. Therefore, a unique aspect of this work has been the direct observation and characterization of the borane products and metastable reaction intermediates by MAS and solution phase ^{11}B NMR studies.

Table 1. Ligand ratios in synthesized solvates, determined by ^1H NMR.

Solvate	Mg:Ligand Ratio
$Mg(BH_4)_2$·DMS §	1:0.34
$Mg(BH_4)_2$·TEA	1:1.8
$Mg(BH_4)_2$·Et_2O	1:0.36
$Mg(BH_4)_2$·Digly	1:1.18
$Mg(BH_4)_2$·DME	1:2.2
$Mg(BH_4)_2$·THF	1:2.8

§ The dimethyl sulfide (DMS) solvate was obtained through the synthetic protocol as described by Zanella et al. [32]. The DMS is weakly bond to the magnesium cation and readily removed by heating.

The TEA, Et_2O, Digly, DME and THF solvates of $Mg(BH_4)_2$, were prepared by adding an excess of solvent to $Mg(BH_4)_2$ at room temperature. Subsequently the solvent was removed *en vacuo* to obtain a crystalline solid. The stoichiometry of the solvates was determined from the relative integrated intensities of the signals observed in the ^{1}H NMR spectra as summarized in Table 1. Where we could find crystal structure information for solvates of $Mg(BH_4)_2$, the stoichiometry of solvate to Mg cation determine by NMR in our work is slightly greater than reported for $Mg(BH_4)_2$·DME 1:1.5 and slightly lower for $Mg(BH_4)_2$·THF 1:3 [33].

Unsolvated $Mg(BH_4)_2$ and solvate powders were dehydrogenated via combinatorial screening equipment made by Unchained Labs® (Pleasanton, CA, USA), consisting of a 24 well plate design. Heating of the samples was conducted in a screening pressure reactor at 180 °C for 24 h under N_2 flow. Product ratios determined by ^{11}B NMR are shown in Table 2. Entry 1 shows the low reactivity of unsolvated $Mg(BH_4)_2$ at 180 °C with 93% BH_4^- remaining. This result is typical of the slow kinetics of dehydrogenation for borohydride complexes at temperatures below 300 °C. Dehydrogenation of the TEA complex favored formation of $B_3H_8^-$, along with a trace amount of $B_{10}H_{10}^{2-}$. The ether additives showed higher levels of dehydrogenation at 180 °C. Another difference found with the ether complexes is the observation of $B_{10}H_{10}^{2-}$ as the major product, suggesting either a competing dehydrogenation path or that the presence of these ether ligands encourages further reactivity of the $B_3H_8^-$ to form more deeply dehydrogenated products. Of the ether solvates, DME and THF provided the highest conversion of BH_4^- with $B_{10}H_{10}^{2-}$ as the major product. Only small amounts of $B_{12}H_{12}^{2-}$, demonstrating that the decomposition was ~10× more selective for $B_{10}H_{10}^{2-}$ than $B_{12}H_{12}^{2-}$, much higher than the ~1.5× selectivity exhibited by the Digly solvate. These findings motivated further exploration of the dehydrogenation reaction.

Table 2. Distribution of products of $Mg(BH_4)_2$ solvates determined from integration of ^{11}B NMR peaks in mol % after dehydrogenation at 180 °C, 24 h, 1 atm N_2. The balance of products consist of trace quantities of boric acid due to hydrolysis of unstable polyboranes.

Sample	$B_{10}H_{10}^{2-}$	$B_3H_8^-$	$B_{12}H_{12}^{2-}$	BH_4^-
$Mg(BH_4)_2$		3		93
$Mg(BH_4)_2$·TEA	2	6		89
$Mg(BH_4)_2$·Et_2O	4	4		88
$Mg(BH_4)_2$·Digl	5	2	3	82
$Mg(BH_4)_2$·DME	46	14	4	30
$Mg(BH_4)_2$·THF	31	12	3	39

3. Discussion

A recent study asserted that closo-boranes are secondary products formed upon aqueous workup of the low temperature dehydrogenation reactions [34]. To determine if formation of $B_{10}H_{10}^{2-}$ occurs directly in the solid state reaction, the ^{11}B VT MAS NMR spectrum of dehydrogenated (1 atm N_2 at 180 °C for 24 h) $Mg(BH_4)_2$·THF was obtained (Figure 1). At room temperature, the observed resonances were broad, typical of solid state spectra for quadrupolar nuclei. Heating the sample to 160 °C sharpened the BH_4^- peak and the resonances for $B_{10}H_{10}^{2-}$ at −2 and −27 ppm could be resolved. The peaks at −2 and −27 ppm assigned to the basal and apical boron in $B_{10}H_{10}$ based on the 1:4 ratio integration ratio in the solid state spectrum at 160 °C. At 20 °C the peaks are barely perceptible from the baseline. The sample is subsequently dissolved in a mixture of THF/D_2O for solution NMR analysis. A solution phase spectrum of the dehydrogenated complex was obtained for comparison of product distribution and line width after dissolution in THF/D_2O (Figure 1c). The same high selectivity for $B_{10}H_{10}^{2-}$ is observed in both solution (−2, −30 ppm) and solid-state NMR with respective yields of 19% and 18%.

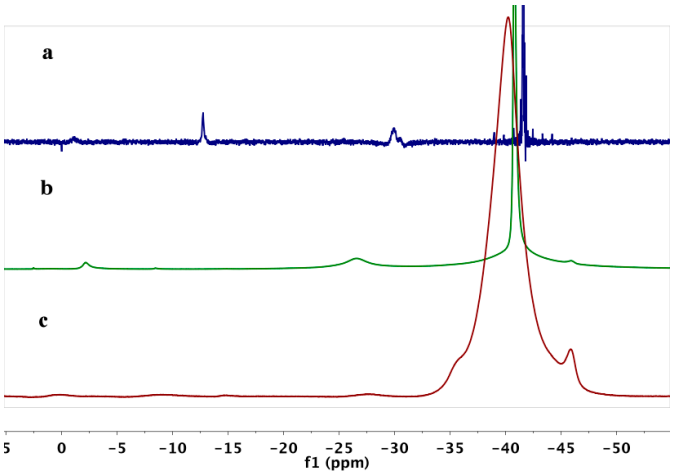

Figure 1. ^{11}B NMR spectra of $Mg(BH_4)_2$·THF (tetrahydofuran) dehydrogenated (**a**) solution phase dissolved in 1:2 THF:D_2O, (**b**) solid state collected at 160 °C and (**c**) solid state collected at 20 °C. Experimental set-up described in references [35,36].

In situ VT MAS ^{11}B NMR studies of the $Mg(BH_4)_2$·THF complex provides additional insight. As seen in Figure S1, the room temperature spectrum contains resonances for both unsolvated and solvated $Mg(BH_4)_2$ at −41 and −44 ppm respectively. See Figure S2 for a reference spectrum of unsolvated $Mg(BH_4)_2$. The downfield shift of the THF solvated BH_4^- complex is comparable to the downfield shift reported for $Mg(BH_4)_2$·$4NH_3$ [37]. Upon heating the two peaks collapse into a single narrow peak at 90 °C. We interpret the narrow line width (FWHM = 32 Hz) as being indicative of a fluid phase. This is consistent with the observation of the melting of the THF solvate between 80–100 °C in a melting point apparatus and similar to the m.p. of 90 °C reported for $Mg(BH_4)_2$·$2NH_3$ [36].

A comparison of the IR spectra of the solvated and unsolvated $Mg(BH_4)_2$ complex is shown in Figure 2. The single prominent stretch observed in the B–H stretching region between 2300–2500 cm^{-1} [38] for $Mg(BH_4)_2$ is indicative of lack of directional bonding between the Mg cation and the tetrahedral environment of BH_4^-. The additional coordination of THF molecules results in the BH_4^- also bonding in a mono or bidentate mode to the Mg cation. This lowering of symmetry leads to a spectrum with a number of overlapping bands occur between 2000–2500 cm^{-1}. The modified coordination may play a role in the dehydrogenation mechanism and energetics.

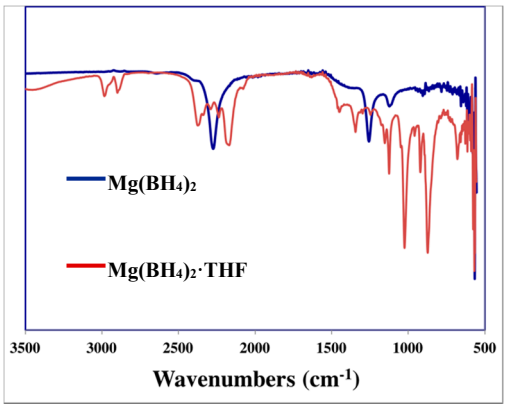

Figure 2. Attenuated Total Reflectance-Infrared spectra of unsolvated $Mg(BH_4)_2$ blue spectra with simple B–H stretching region and $Mg(BH_4)_2$·THF red spectrum with complex B–H stretching frequency.

The melting of the THF adduct is also likely to be a contributing factor to the enhanced kinetics. However, the onset of dehydrogenation occurs at temperatures above the melting point of the

THF complex. The THF may also reduce the activation energy of clustering to form more deeply dehydrogenated products by altering the coordination mode between Mg^{2+} and BH_4^- through donation of electron density or steric interactions. The high selectivity for $MgB_{10}H_{10}$ over $MgB_{12}H_{12}$ is surprising. Either THF influences the reaction pathway, i.e., lower the barrier for a branching point that pushes the reaction towards $MgB_{10}H_{10}$ formation or THF flips the thermodynamic stability of the closoboranes making $MgB_{10}H_{10}$ more stable than $MgB_{12}H_{12}$.

4. Materials and Methods

All sample preparation and storage was conducted either in a nitrogen glovebox or on a Schlenk line. Solvents were dried over molecular sieves and verified by NMR for purity before use.

4.1. Synthesis of $Mg(BH_4)_2$

Magnesium borohydride was synthesized following a method described by Zanella et al. Di-*n*-butylmagnesium (Sigma Aldrich, Milwaukee, WI, USA) was added dropwise to borane-dimethylsulfide complex (Sigma Aldrich) in toluene according to the reaction scheme:

$$3Mg(C_4H_9)_2 + 8BH_3{\cdot}S(CH_3)_2 \rightarrow 3Mg(BH_4)_2{\cdot}2S(CH_3)_2 + 2B(C_4H_9)_3{\cdot}S(CH_3)_2$$

The mixture was allowed to stir at room temperature for a minimum of 3 h and subsequently filtered, washed with toluene, and dried *en vacuo* at room temperature for 6 h and then at 75 °C overnight. The product, a fine white powder, was found to consist of >95% α-$Mg(BH_4)_2$ by XRD analysis.

4.2. Synthesis of Solvent Adducts of $Mg(BH_4)_2$

The TEA, Et_2O, Digly, and THF solvates of $Mg(BH_4)_2$, were typically prepared by adding an excess of solvent to $Mg(BH_4)_2$ at room temperature and stirring for 30 min. Excess solvent was then removed *en vacuo* either at room temperature or up to 45 °C for higher boiling point solvents, for as long as needed to obtain a crystalline solid. The DMS adduct was obtained during the synthesis of $Mg(BH_4)_2$ as described above prior to removal of the DMS by heating.

4.3. Characterization of $Mg(BH_4)_2$ Adducts and Decomposition Products by Solution NMR

Powders were typically dissolved in a 1:2 mixture of THF:deuterium oxide (D_2O) and analyzed within 10 min on a Varian 300 MHz spectrometer with ^{11}B chemical shifts referenced to $BF_3{\cdot}Et_2O$ (δ = 0 ppm) and ^1H referenced to TMS (δ = 0 ppm). ^{11}B was measured at 96.23 MHz and ^1H was measured at 299.95 MHz. A relaxation delay of 15 s was used for all ^{11}B analyses with a 90° pulse width of 6 µs. An external standard was added to the quartz NMR tubes to determine the solubility of the powder in the THF/D_2O mixture. The standard consisted of an aqueous solution of sodium tetraphenylborate ($NaBPh_4$) sealed in a glass capillary. Calculation of percent composition of decomposed products was based on peak areas.

4.4. Solid State NMR

Sample powders were packed into 4 mm zirconium oxide rotors and spun at 12 kHz on a Varian 500 MHz spectrometer (Varian, Palo Alto, CA, USA) equipped with a HX 4 mm probe.

4.5. In Situ NMR

The characterization of $Mg(BH_4)_2{\cdot}THF$ during heating to 200 °C was conducted by variable temperature (VT) solid state magic angle spin (MAS) NMR in a Varian 500 MHz spectrometer 5 mm HXY probe. ^1H and ^{11}B shifts were referenced to tetramethylsilane at 0 ppm and lithium borohydride at −41.6 ppm and measured at 499.87 and 160.37 MHz respectively. ^1H and ^{11}B spectra were obtained with a 2 s and 5 s relaxation delay and 90° pulse width of 6 µs. The sample powder was packed in a

5 mm zirconia rotor under 1 atm N_2 with a Teflon spacer and then capped with a customized plastic bushing capable of withstanding pressures up to 200 bar. The details of the rotor design are given in detail elsewhere [32,33] and have been modified to accommodate 5 mm rotors. The rotors were spun at 5 kHz at room temperature and subsequently heated at a rate of about 6 °C/min and held at specific temperatures during the ramp at which ^{11}B and ^{1}H spectra were obtained. The duration of the analyses at the set temperatures was approximately 45 min.

5. Conclusions

In summary, characterization of the dehydrogenation products arising from $Mg(BH_4)_2 \cdot THF$ complex by solution and solid-state NMR shows that the dehydrogenation mechanism is highly selective for $B_{10}H_{10}^{2-}$ over $B_3H_8^-$ (theoretical H_2 release 8.1 wt % vs. 2.5 wt % in the absence of solvates) and $B_{12}H_{12}^{2-}$, a kinetic dead end. The dehydrogenation of $Mg(BH_4)_2$ at temperatures below 200 °C and potential for cycling between $Mg(BH_4)_2$ and $MgB_{10}H_{10}$ have significant implications for hydrogen storage applications. Further studies into optimizing the reaction through modification of ligand to Mg ratios are currently underway.

Supplementary Materials: The following are available online at www.mdpi.com/2304-6740/5/4/89/s1, Figure S1: In situ VT MAS ^{11}B NMR of $Mg(BH_4)_2 \cdot THF$ at room temperature and 90 °C. Figure S2: ^{11}B MAS spectra of unsolvated $Mg(BH_4)_2$ and solvated $Mg(BH_4)_2 \cdot THF$.

Acknowledgments: The authors gratefully acknowledge research support from the Hydrogen Materials—Advanced Research Consortium (HyMARC), established as part of the Energy Materials Network under the U.S. Department of Energy, Office of Energy Efficiency and Renewable Energy, Fuel Cell Technologies Office. We authors thank Junzhi Yang for preliminary experimental results on solvated magnesium borane complexes, Heather Job for assistance with the combinatorial decomposition experiments, Gary Edvenson for insightful discussion on borane cluster chemistry and David Hoyt and Sarah Burton from the Environmental Molecular Science Laboratory (EMSL) for assistance with the solid state NMR. EMSL is a DOE Office of Science User Facility sponsored by the Office of Biological and Environmental Research and located at Pacific Northwest National Laboratory (PNNL). PNNL a multi-program national laboratory operated by Battelle for the U.S. Department of Energy under Contract DE-AC05-76RL01830.

Author Contributions: Marina Chong, Tom Autrey and Craig Jensen conceived and designed the experiments; Marina Chong performed the experiments; Marina Chong, Tom Autrey and Craig Jensen contributed to analyzing the data and writing the paper.

Conflicts of Interest: The authors declare no conflict of interest.

References

1. Chong, M.; Karkamkar, A.; Autrey, T.; Orimo, S.; Jalisatgi, S.; Jensen, C.M. Reversible dehydrogenation of magnesium borohydride to magnesium triborane in the solid state under moderate conditions. *Chem. Commun.* **2011**, *47*, 1330–1332. [CrossRef]
2. Filinchuk, Y.; Richter, B.; Jensen, T.R.; Dmitriev, V.; Chernyshov, D.; Hagemann, H. Porous and dense magnesium borohydride frameworks: Synthesis, stability, and reversible absorption of guest species. *Angew. Chem. Int. Ed.* **2011**, *50*, 11162–11166. [CrossRef]
3. Hanada, N.; Chłopek, K.; Frommen, C.; Lohstroh, W.; Fichtner, M. Thermal decomposition of $Mg(BH_4)_2$ under He flow and H_2 pressure. *J. Mater. Chem.* **2008**, *18*, 2611–2614. [CrossRef]
4. Hwang, S.-J.; Bowman, R.C., Jr.; Reiter, J.W.; Rijssenbeek, J.; Soloveichik, G.; Zhao, J.-C.; Kabbour, H.; Ahn, C.C. NMR confirmation for formation of $[B_{12}H_{12}]^{2-}$ complexes during hydrogen desorption from metal borohydrides. *J. Phys. Chem. C* **2008**, *112*, 3164–3169. [CrossRef]
5. Li, H.-W.; Kikuchi, K.; Sato, T.; Nakamori, Y.; Ohba, N.; Aoki, M.; Miwa, K.; Towata, S.; Orimo, S. Synthesis and hydrogen storage properties of a single-phase magnesium borohydride $Mg(BH_4)_2$. *Mater. Trans.* **2008**, *49*, 2224–2228. [CrossRef]
6. Matsunaga, T.; Buchter, F.; Mauron, P.; Bielman, M.; Nakamori, Y.; Orimo, S.; Ohba, N.; Miwa, K.; Towata, S.; Züttel, A. Hydrogen storage properties of $Mg[BH_4]_2$. *J. Alloys Compd.* **2008**, *459*, 583–588. [CrossRef]

7. Nakamori, Y.; Miwa, K.; Ninomiya, A.; Li, H.-W.; Ohba, N.; Towata, S.; Züttel, A.; Orimo, S. Correlation between thermodynamical stabilities of metal borohydrides and cation electronegativites: First-principles calculations and experiments. *Phys. Rev. B* **2006**, *74*, 045126. [CrossRef]
8. Ozolins, V.; Majzoub, E.H.; Wolverton, C. First-principles prediction of a ground state crystal structure of magnesium borohydride. *Phys. Rev. Lett.* **2008**, *100*, 135501. [CrossRef]
9. Severa, G.; Ronnebro, E.; Jensen, C.M. Direct hydrogenation of magnesium boride to magnesium borohydride: Demonstration of >11 weight percent reversible hydrogen storage. *Chem. Commun.* **2010**, *46*, 421–423. [CrossRef]
10. Van Setten, M.J.; de Wijs, G.A.; Fichtner, M.; Brocks, G.A. A Density Functional Study of alpha-$Mg(BH_4)_2$. *Chem. Mater.* **2008**, *20*, 4952–4956. [CrossRef]
11. Yan, Y.; Li, H.-W.; Nakamori, Y.; Ohba, H.; Miwa, K.; Towata, S.; Orimo, S. Differential scanning calorimetry measurements of magnesium borohydride $Mg(BH_4)_2$. *Mater. Trans.* **2008**, *49*, 2751–2752. [CrossRef]
12. Zavorotynska, O.; Deledda, S.; Hauback, B.C. Kinetics studies of the reversible partial decomposition reaction in $Mg(BH_4)_2$. *Int. J. Hydrog. Energy* **2016**, *41*, 9885–9892. [CrossRef]
13. Zhang, Y.; Majzoub, E.; Ozoliņš, V.; Wolverton, C. Theoretical prediction of metastable intermediates in the decomposition of $Mg(BH_4)_2$. *J. Phys. Chem. C* **2012**, *116*, 10522–10528. [CrossRef]
14. Chłopek, K.; Frommen, C.; Léon, A.; Zabara, O.; Fichtner, M. Synthesis and properties of magnesium tetrahydroborate, $Mg(BH_4)_2$. *J. Mater. Chem.* **2007**, *17*, 3496–3503. [CrossRef]
15. Li, H.-W. Dehydriding and rehydriding processes of well-crystallized $Mg(BH_4)_2$ accompanying with formation of intermediate compounds. *Acta Mater.* **2008**, *56*, 1342–1347. [CrossRef]
16. White, J.L.; Newhouse, R.J.; Zhang, J.Z.; Udovic, T.J.; Stavila, V. Understanding and mitigating the effects of stable dodecahydro-closo-dodecaborate intermediates on hydrogen-storage reactions. *J. Phys. Chem. C* **2016**, *120*, 25725–25731. [CrossRef]
17. Li, H.-W.; Kikuchi, K.; Nakamori, Y.; Miwa, K.; Towata, S.; Orimo, S. Effects of ball milling and additives on dehydriding behaviors of well-crystallized $Mg(BH_4)_2$. *Scr. Mater.* **2007**, *57*, 679–682. [CrossRef]
18. Bardají, E.G.; Hanada, N.; Zabara, O.; Fichtner, M. Effect of several metal chlorides on the thermal decomposition behaviour of α-$Mg(BH_4)_2$. *Int. J. Hydrog. Energy* **2011**, *36*, 12313–12318. [CrossRef]
19. Newhouse, R.J.; Stavila, V.; Hwang, S.-J.; Klebanoff, L.; Zhang, J.Z. Reversibility and improved hydrogen release of magnesium borohydride. *J. Phys. Chem. C* **2010**, *114*, 5224–5234. [CrossRef]
20. Saldan, I.; Frommen, C.; Llamas-Jansa, I.; Kalantzopoulos, G.N.; Hino, S.; Arstad, B.; Heyn, R.H.; Zavorotynska, O.; Deledda, S.; Sørby, M.H.; et al. Hydrogen storage properties of γ–$Mg(BH_4)_2$ modified by MoO_3 and TiO_2. *Int J. Hydrog. Energy* **2015**, *40*, 12286–12293. [CrossRef]
21. Bardají, E.G.; Zhao-Karger, Z.; Boucharat, N.; Nale, A.; van Setten, M.J.; Lohstroh, W.; Röhm, E.; Catti, M.; Fichtner, M. $LiBH_4-Mg(BH_4)_2$: A physical mixture of metal borohydrides as hydrogen storage material. *J. Phys. Chem. C* **2011**, *115*, 6095–6101. [CrossRef]
22. Hagemann, H.; D'Anna, V.; Rapin, J.-P.; Černý, R.; Filinchuk, Y.; Kim, K.C.; Sholl, D.S.; Parker, S.T. New fundamental experimental studies on α-$Mg(BH_4)_2$ and other borohydrides. *J. Alloys Compd.* **2011**, *509*, S688–S690. [CrossRef]
23. Nale, A.; Catti, M.; Bardají, E.G.; Fichtner, M. On the decomposition of the $0.6LiBH_4$–$0.4Mg(BH_4)_2$ eutectic mixture for hydrogen storage. *Int. J. Hydrog. Energy* **2011**, *36*, 13676–13682. [CrossRef]
24. Yang, J.; Fu, H.; Song, P.; Zheng, J.; Li, X. Reversible dehydrogenation of $Mg(BH_4)_2$–LiH composite under moderate conditions. *Int. J. Hydrog. Energy* **2012**, *37*, 6776–6783. [CrossRef]
25. Muetterties, E.L.; Knoth, W.H. *Polyhedral Boranes*; Marcel Dekker: New York, NY, USA, 1968.
26. Chong, M.; Matsuo, M.; Orimo, S.; Autrey, T.; Jensen, C.M. Selective reversible hydrogenation of $Mg(B_3H_8)_2/MgH_2$ to $Mg(BH_4)_2$: Pathway to reversible borane-based hydrogen storage? *Inorg. Chem.* **2015**, *54*, 4120–4125. [CrossRef]
27. Chen, J.; Chua, Y.S.; Wu, H.; Xiong, Z.; He, T.; Zhou, W.; Ju, X.; Yang, M.; Wu, G.; Chen, P. Synthesis, structures and dehydrogenation of magnesium borohydride–ethylenediamine composites. *Int. J. Hydrog. Energy* **2015**, *40*, 412–419. [CrossRef]
28. Yang, Y.; Liu, Y.; Zhang, Y.; Li, Y.; Gao, M.; Pan, H. Hydrogen storage properties and mechanisms of $Mg(BH_4)_2{\cdot}2NH_3$–$xMgH_2$ combination systems. *J. Alloys Compd.* **2014**, *585*, 674–680. [CrossRef]

29. Zhao, S.; Xu, B.; Sun, N.; Sun, Z.; Zeng, Y.; Meng, L. Improvement in dehydrogenation performance of $Mg(BH_4)_2{\cdot}2NH_3$ doped with transition metal: First-principles investigation. *Int. J. Hydrog. Energy* **2015**, *40*, 8721–8731. [CrossRef]
30. Soloveichik, G.; Her, J.H.; Stephens, P.W.; Gao, Y.; Rijssenbeek, J.; Andrus, M.; Zhao, J.-C. Ammine magnesium borohydride complex as a New material for hydrogen storage: Structure and properties of $Mg(BH_4)_2{\cdot}2NH_3$. *Inorg. Chem.* **2008**, *47*, 4290–4298. [CrossRef]
31. Zavorotynska, O.; El-Kharbachi, A.; Deledda, S.; Hauback, B.C. Recent progress in magnesium borohydride $Mg(BH_4)_2$: Fundamentals and applications for energy storage. *Int. J. Hydrog. Energy* **2016**, *41*, 14387–14404. [CrossRef]
32. Zanella, P.; Crociani, L.; Masciocchi, N.; Giunchi, G. Facile high-yield synthesis of pure, crystalline $Mg(BH_4)_2$. *Inorg. Chem.* **2007**, *46*, 9039–9041. [CrossRef]
33. Wegner, W.; Jaroń, T.; Dobrowolski, M.A.; Dobrzycki, Ł.; Cyrański, M.K.; Grochala, W. Organic derivatives of $Mg(BH_4)_2$ as precursors towards MgB_2 and novel inorganic mixed-cation borohydrides. *Dalton Trans.* **2016**, *45*, 14370–14377. [CrossRef]
34. Yan, Y.; Remhof, A.; Rentsch, D.; Züttel, A. The role of $MgB_{12}H_{12}$ in the hydrogen desorption process of $Mg(BH_4)_2$. *Chem. Commun.* **2015**, *51*, 700–702. [CrossRef]
35. Hoyt, D.W.; Turcu, R.V.F.; Sears, J.A.; Rosso, K.; Burton, S.D.; Felmy, A.R.; Hu, J.-Z. High-pressure magic angle spinning nuclear magnetic resonance. *J. Magn. Res.* **2011**, *212*, 378–385. [CrossRef]
36. Turcu, R.V.F.; Hoyt, D.W.; Rosso, K.M.; Sears, J.A.; Loring, J.S.; Felmy, A.R.; Hu, J.-Z. Rotor design for high pressure magic angle spinning nuclear magnetic resonance. *J. Magn. Res.* **2013**, *226*, 64–69. [CrossRef]
37. Gao, L.; Guo, Y.H.; Li, Q.; Yu, X.B. The comparison in dehydrogenation properties and mechanism between $MgCl_2(NH_3)/LiBH_4$ and $MgCl_2(NH_3)/NaBH_4$ systems. *J. Phys. Chem. C* **2010**, *114*, 9534–9540. [CrossRef]
38. Marks, T.J.; Kolb, J.R. Covalent transition metal, lanthanide, and actinide tetrahydroborate complexes. *Chem. Rev.* **1977**, *77*, 263–293.